

Ion Transport Studies and Determination of the Cell Wall Elastic Modulus in the Marine Alga *Halicystis parvula*

JAMES S. GRAVES and JOHN GUTKNECHT

From the Department of Physiology and Pharmacology, Duke University Medical Center, Durham, North Carolina 27710 and the Duke University Marine Laboratory, Beaufort, North Carolina 28516. Dr. Graves' present address is the Ontario Cancer Institute, Toronto, Ontario, Canada.

ABSTRACT Using cultured cells of the marine alga, *Halicystis parvula*, we measured the concentrations of 11 inorganic ions in the vacuolar sap and the electrical potential difference (PD) between the vacuole and the external solution. In normal cells under steady-state conditions a comparison of the electrochemical equilibrium (Nernst) potential for each ion with the PD of -82 mV (inside negative) indicates that Na^+ and K^+ are actively transported out of the vacuole whereas all anions are pumped into the cell. Although the $[\text{K}^+]$ in the vacuole is only 9 mM, the cytoplasmic $[\text{K}^+]$ is about 420 mM, which suggests that the outwardly directed pump is at the tonoplast. Using large *Halicystis* cells we perfused the vacuole with an artificial seawater and conducted a short-circuit analysis of ion transport. The short-circuit current (SCC) of $299 \text{ pEq} \cdot \text{cm}^{-2} \cdot \text{s}^{-1}$ is not significantly different from the net influx of Cl^- . There is a small, but statistically significant net efflux of K^+ ($<1 \text{ pEq} \cdot \text{cm}^{-2} \cdot \text{s}^{-1}$), while the influx and efflux of Na^+ are not significantly different. Therefore, the SCC is a good measure of the activity of the Cl^- pump. Finally, we measured the volumetric elastic modulus (ϵ) of the cell wall by measuring the change in cell volume when the internal hydrostatic pressure was altered. The value of ϵ at applied pressures between 0 and 0.4 atm is about 0.6 atm, which is at least 100-fold lower than the values of ϵ for all other algae which have been studied.

INTRODUCTION

The large single-celled alga, *Halicystis*, has played an important historical role in the development of our current understanding of ion transport processes and bioelectrical phenomena. In their early investigations Blinks and coworkers studied the bioelectric properties and the distributions of inorganic ions between the vacuole and external seawater in two species of *Halicystis*. While both species had similar electrical potentials (-60 to -80 mV, inside negative), the ratios of Na^+ to K^+ in the vacuolar sap were very different. In *Halicystis ovalis*, the Pacific Coast species, the concentrations of Na^+ and K^+ in the sap were both about 300 mM (4). However, in *Halicystis osterhoutii* from Bermuda the $[\text{Na}^+]$ in the sap was about 100 times the concentration of K^+ (2).

None of the contemporary studies on ion transport in marine algae has dealt with a species in which the vacuolar sap is similar in ionic composition to the

external seawater (e.g., *H. osterhoutii*). The mechanisms involved in maintaining this type of ionic distribution must be different from those of *H. ovalis* (3) or any of the other algal species previously studied (18). Furthermore, the large size of *Halicystis* cells provides the opportunity to perfuse the vacuole and thus use the short-circuit analysis of ion transport. Therefore, a thorough study of the ion transport properties of this type of alga seemed warranted.

Given the lack of availability of *H. osterhoutii*, we found a species with similar sap composition, *Halicystis parvula*, which has been maintained in unialgal culture for several years. Since the ionic relations of this alga have not previously been described, our initial step was to thoroughly describe the ionic composition of the vacuolar sap and to measure the electrical properties of the cell. From these data an analysis using the Nernst equation revealed the existence and direction of any active ion transport. Using internally perfused cells we also measured the short-circuit current and the net fluxes of Na^+ , K^+ , and Cl^- in order to further characterize and quantify the transport processes for these ions. Finally, the large volume changes which accompanied changes in turgor pressure led us to measure the elastic modulus of the cell wall, which is an important parameter in the osmotic relations of a plant cell (6).

Halicystis exists as a single, multinucleate cell (i.e., coenocyte) which is classified in the order Siphonales (5). Kornmann (26) found that *Halicystis* and the finely filamentous alga, *Derbesia*, were actually alternating generations in the life cycle of the same organism. Fig. 1 shows the general pattern of the *Derbesia-Halicystis* life cycle. The *Halicystis* vesicle constitutes the gametophytic stage of

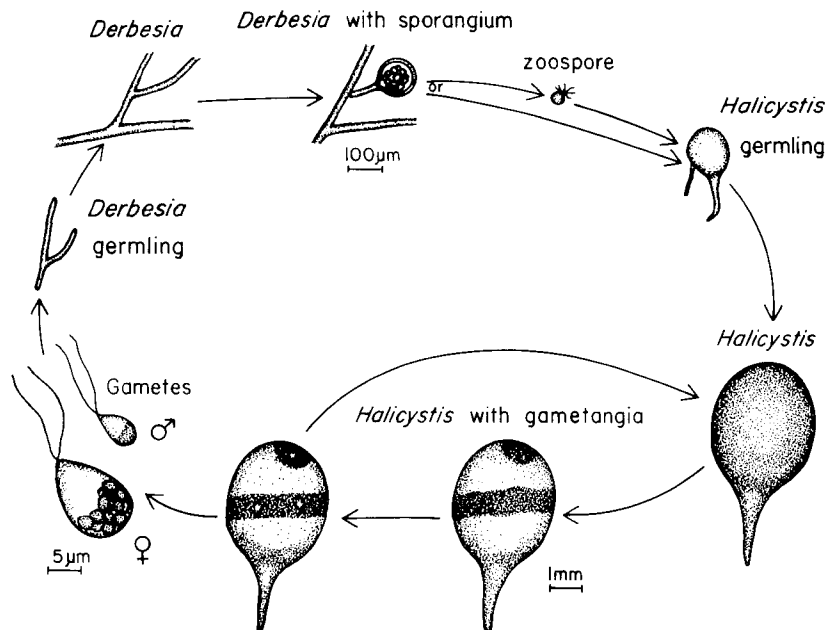


FIGURE 1. The life-cycle of *Derbesia-Halicystis*. Data incorporated from Ziegler and Kingbury (48), Sears and Wilce (38) in addition to our own observations.

this cycle. Because the identification of *Derbesia* predates by 4 yr the identification of *Halicystis*, the technically proper name of the alga is *Derbesia* (31). However, we will use the name *Halicystis* in order to avoid confusion with the literature on ion transport in which the name *Halicystis* has been used exclusively.

METHODS

Culture and General Experimental Conditions

Initial cultures of *Derbesia-Halicystis* were obtained from Carolina Biological Supply Co., Burlington, N. C. The culture medium was natural seawater collected at least 3 miles off the North Carolina coast and adjusted to 3.3% salinity by addition of either a concentrated seawater brine or H₂O. Before use the seawater was twice heated to at least 90°C and, after cooling, enriched with 20 ml/liter Alga-Gro nutrient concentrate (Carolina Biological Supply Co.). Cultures were maintained in sterilized, Pyrex storage dishes in 200-300 ml of enriched seawater (ESW) and were kept in a growth chamber at 19-21°C with a daily light-dark cycle of 18:6. The average light intensity during light periods, measured with YSI-Kettering Radiometer (Yellow Springs Instrument Co., Yellow Springs, Ohio), was 10 joule (J) · m⁻² · s⁻¹. The ESW was renewed every 3-4 wk. Under these conditions the organisms grew well and were reproductive.

Experiments were conducted with cells not obviously undergoing gametogenesis. The artificial seawater (ASW) had the following composition (mM): 450 NaCl, 10 KCl, 10 CaCl₂, 25 MgCl₂, 26.5 MgSO₄, 2.5 NaHCO₃, 1.0 NaBr, 0.1 NaNO₃, 0.05 Na₂HPO₄, pH 7.9-8.0. From measurements on six batches of ASW the osmolality was 990 ± 5 mosmol/kg (mean ± SE), which corresponds to a salinity of approximately 3.3%. Before each experiment cells were preincubated in ASW for at least 24 h at 21°C with constant illumination (ca. 4 J · m⁻² · s⁻¹). Under these conditions, the cells appeared healthy and grew well for at least 1 wk. Experiments were conducted at room temperature (21-23°C).

The *Halicystis* vesicles used in this study were assumed to have either of the two characteristic shapes shown in Fig. 2. For smaller cells (*b* < 3 mm), shape I predominated, but as cells grew larger, shape II became more common. The sphere formulae for shape II were used when *a-b* < 1 mm. Otherwise the shape I formulae, which combine those for

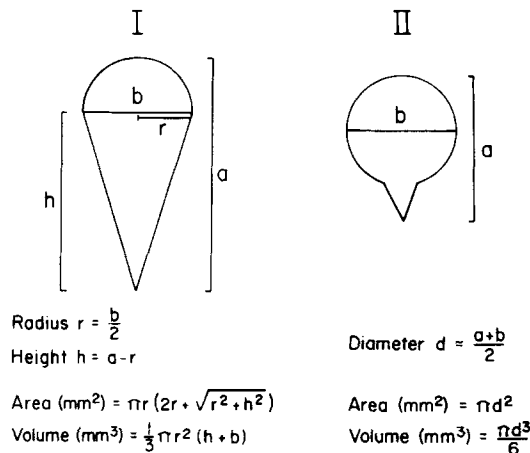


FIGURE 2. Characteristic shapes of *H. parvula* cells and the formulae used to compute surface area and volume.

a cone and a hemisphere, were used. Using these criteria we found a good correlation between the measured volume and the mass of intracellular water. Dimensions were measured with a 15-cm ruler under $\times 2$ magnification. Cells used in this study had a wide range of sizes ($b = 2-6$ mm).

Ion Concentration and Osmolality Measurements

Pure vacuolar sap was collected by impaling the cell with a micropipet and withdrawing the sap by suction. Except where indicated, cells used for this purpose had a size range of $b = 2-3$ mm. Micropipets were pulled from Pyrex glass tubing (OD = 1.90 mm, ID = 1.4 mm) with a Kopf vertical puller (David Kopf Instruments, Tiyunga, Calif., model 700 C). The tips were externally siliconized by dipping into a 2% (vol/vol) solution of Siliclad (Clay Adams Div. of Becton, Dickinson & Co., Parsippany, N.J.) in 2,4-dichloroethane and heating at greater than 90°C for at least 1 h. Before use the tip was broken off to 50–100 μm , and the pipet was then connected to an oil-filled 0.2-ml Gilmont micrometer syringe with PE 200 tubing. The oil was colored by adding a few grains of Sudan Black dye. Once assembled and filled with oil the pipet was inserted into the cell and the clear sap withdrawn. A measured aliquot of sap was then expelled into an appropriate container. By weighing measured aliquots of 20°C water the accuracy of this device was determined to be about 0.95 times ideal, and this correction was made.

The concentrations of Na^+ and K^+ were determined by atomic absorption spectrophotometry (Varian AA-6, Varian Associates, Palo Alto, Calif.) using an air-acetylene flame. Single-cell sap samples of 4–12 μl and standards were diluted in 4.0 mM CsCl, which suppresses ionization interferences (37).

Whole-cell K^+ concentration was determined in the following manner. Cells were rinsed in K-free ASW for 30–60 s, carefully blotted and weighed. Each cell was placed in a tube with 4.0 ml of 4.0 mM CsCl_2 , freeze-thawed twice, and directly assayed for K^+ . In separate experiments the percent cell water was determined by weighing cells after blotting and again after drying for 5 h at 100–110°C. The value from 11 such determinations was $95.0 \pm 0.4\%$ water. This correction was used to compute the intracellular $[\text{K}^+]$ in millimoles per liter cell H_2O .

The concentrations of Ca^{++} and Mg^{++} were also determined by atomic absorption spectrophotometry using a nitrous oxide-acetylene flame for Ca^{++} and an air-acetylene flame for Mg^{++} . Single-cell sap samples of 5–10 μl and standards were diluted in 20.0 mM LaCl_3 , which suppresses anion interferences (37). Standards were made from anhydrous CaCl_2 and a commercial solution of Mg acetate (Varian-Techtron).

Chloride concentration was determined by coulometric titration with a Buchler-Cotlove Chloridometer (Buchler Instruments Div., Searle Analytic Inc., Fort Lee, N.J.). Single-cell sap samples of 4–10 μl were placed directly into titration vials for assay.

Nitrate concentrations were determined by a modification of the method of Lowe and Evans (29). Nitrate is reduced to nitrite with *Escherichia coli* nitrate reductase (Worthington Biochemical Corp., Freehold, N.J.) and the $[\text{NO}_2^-]$ is subsequently determined by colorimetric analysis (14). Since the ESW $[\text{NO}_3^-]$ was about five times that of ASW, the cells were incubated for 3–4 days in ASW in order to reach a new steady-state concentration before determining the sap $[\text{NO}_3^-]$.

The concentration of sap phosphate was determined on pooled 50–150- μl samples. The assay procedure was similar to that originally developed by Fiske and Subbarow (9) and is described in detail by Graves (14).

The concentrations of Br^- and $\text{SO}_4^{=}$ were estimated by equilibration with external radioisotopes. High specific activity $^{82}\text{Br}^-$ was purchased from ICN as NaBr. Specific activity equilibration was experimentally found to require about 48 h. Sulfate-35 was

purchased from New England Nuclear (Boston, Mass.) as Na_2SO_4 (625 mCi/mmol). The time required for the $^{35}\text{SO}_4^-$ to equilibrate was about 8 days. In both cases comparison of the external specific activity with the count rate for isolated sap yielded the apparent sap concentration of the ion in question.

Phosphate and SO_4^- are both metabolized, and thus the organic forms of either may exist in the vacuolar sap. Since the assay method for each may have measured both organic and inorganic forms, it was necessary to determine the percent inorganic. The two forms were separated by paper chromatography using the solvent system, 40 ml *t*-butanol, 10 ml H_2O , 2 g picric acid, shown by Hanes and Ischerwood (19) to give the best separation of phosphate esters. Sap from cells equilibrated with ASW containing $\text{H}^{32}\text{PO}_4^-$ or $^{35}\text{SO}_4^-$ was chromatographed on Whatman 1 chromatography paper (Whatman Inc., Clifton, N.J.) (2.0 cm wide, medium flow rate), and after air drying 1-cm segments of the chromatogram were counted with an end-window counter. (Liquid scintillation counting was impossible because of picric acid quenching.) In order to identify any organic components, the peaks of radioactivity in the sap were compared with those due to the inorganic isotopes which were run separately.

The pH of the vacuolar sap was determined on 0.1–0.2-ml samples pooled from several large cells ($b = 3\text{--}4.5$ mm). A small-tipped combination pH electrode (MI-410, Microelectrodes, Inc., Londonderry, N. H.), which requires only 1.5-mm immersion depth, was attached to a standard pH meter. The pH measurements were made immediately after collection, although no change was observed after exposure to air. The electrode was standardized with a commercial pH 4 buffer.

The pooled sap samples used for pH measurements were immediately reappportioned into 0.2-ml samples and used to determine the osmolality with a freezing-point depression Advanced Osmometer (Advanced Instruments, Inc., Needham Heights, Mass.). In a separate experiment sap samples were pooled solely for the purpose of determining osmolality. The sap osmolality values were compared to the values for the ASW in which they were growing (not the mean ASW osmolality) for an estimation of the osmotic pressure difference, i.e. turgor pressure.

Electrical Measurements with Microelectrodes

The electrical potential difference (PD) and the surface resistance (R_s) between the vacuole and external solution were measured with the system shown in Fig. 3. Glass capillary microelectrodes were pulled from Pyrex tubing (OD = 2.0 mm, ID = 1.0 mm) to a tip diameter of about 1 μm and were filled with 2.5 M filtered NaCl by vacuum boiling. (Sodium chloride was used instead of KCl because of the low vacuolar $[\text{K}^+]$.) These electrodes had 1–10-M Ω resistances and –5- to +10-mV tip asymmetries. The reference electrode was a glass pipet with a 0.2–0.3-mm tip diameter and filled with 2.5 M NaCl-2% agar. Connections to the measuring circuit were made with Ag-AgCl wires.

Each cell was routinely impaled with two microelectrodes attached to micromanipulators. The PD was measured in each circuit by a high impedance device in series with a Brush Mark 220 two-channel recorder. Both the Keithley Electrometer (Keithley Instruments, Inc., Cleveland, Ohio, model 600B) and the unity-gain preamplifier (constructed with Analog Device 503J operational amplifier, Analog Devices, Inc., Norwood, Mass.) had input impedances of at least 10^{11} Ω . To measure R_s an electrical stimulator (American Electronic Laboratories, Inc., Lansdale, Pa., model 751-B) in series with a constant current device (see 12, for description) provided a desired constant current irrespective of any changes in the electrode or cell resistance.

Before an electrical experiment the cell dimensions were measured, and then the cell was secured with dental wax to a small Lucite stage. This stage was placed in a Lucite

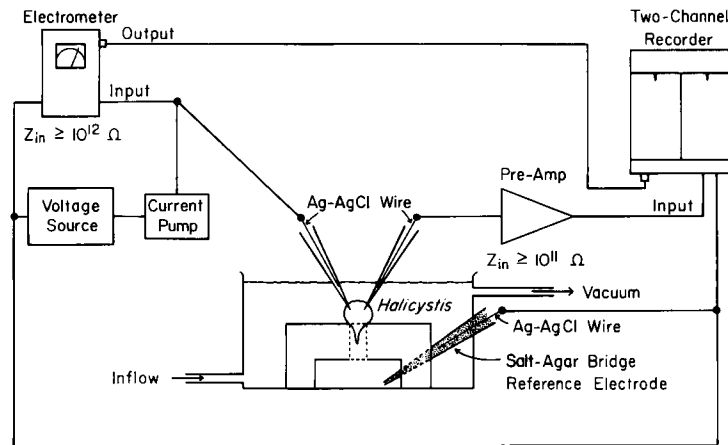


FIGURE 3. Diagram of system used for measuring the electrical properties of *H. parvula* cells.

chamber through which ASW was perfused by gravity flow and vacuum aspiration. Before impalement the desired current was applied and the small voltage deflection, which is a function of the bath and reference electrode resistances, was recorded to be later subtracted from the cell resistance measurement. The cell was impaled with the aid of a dissecting microscope and was illuminated ($15\text{--}20 \text{ J} \cdot \text{m}^{-2} \cdot \text{s}^{-1}$) via a fiber-optic "light-wire" originating from a microscope lamp outside the Faraday cage. The current electrode was driven far into the vacuole to minimize any error resulting from cable properties of the cell. After impalement the PD was continuously recorded and the cell resistance was measured periodically with 1-s hyperpolarizing square pulses of either 0.4 or 1.0 μA . The surface resistance ($\text{ohm} \cdot \text{cm}^2$) was calculated from Ohm's law.

Vacuolar Perfusion and Voltage Clamp

The system diagrammed in Fig. 4 was used when voltage control and vacuolar perfusion were desired. The perfusion pipets were siliconized and beveled on a rotating corundum surface (No. 600) to a tip diameter of 90–110 μm . The cell was first measured ($b = 4.5\text{--}6.0 \text{ mm}$) and then secured with dental wax to the bottom of a Lucite chamber. With both perfusion tubes closed the inflow pipet was rapidly thrust through the cell wall with the aid of a micromanipulator and a vertically oriented dissecting microscope. After the cytoplasm had visibly sealed around the first pipet (usually less than 5 min), the outflow pipet was forced through the cell wall. If a cell suffered obviously severe damage during the impalement procedure, it was discarded. However, the wound usually healed quickly, and the PD became normal (-60 to -80 mV) within 30 min. To perfuse the vacuole the inflow reservoir was raised 20–24 cm above the outflow reservoir, which usually provided a perfusion rate of 2.0–2.4 ml/h.

The cell PD was changed to the desired level with the voltage control device (i.e., voltage clamp) shown in Fig. 4. This device was designed and constructed by Mr. John Adams of the Department of Physiology and Pharmacology, and the circuit diagram is shown elsewhere (14). During the course of an experiment both the PD and current output of the voltage clamp were displayed on a two-channel recorder.

Ion Fluxes in Internally Perfused Cells

The unidirectional fluxes of Na^+ , K^+ , and Cl^- were measured with ASW on both sides of the cytoplasm and the PD clamped at zero (i.e., short-circuit conditions). The following

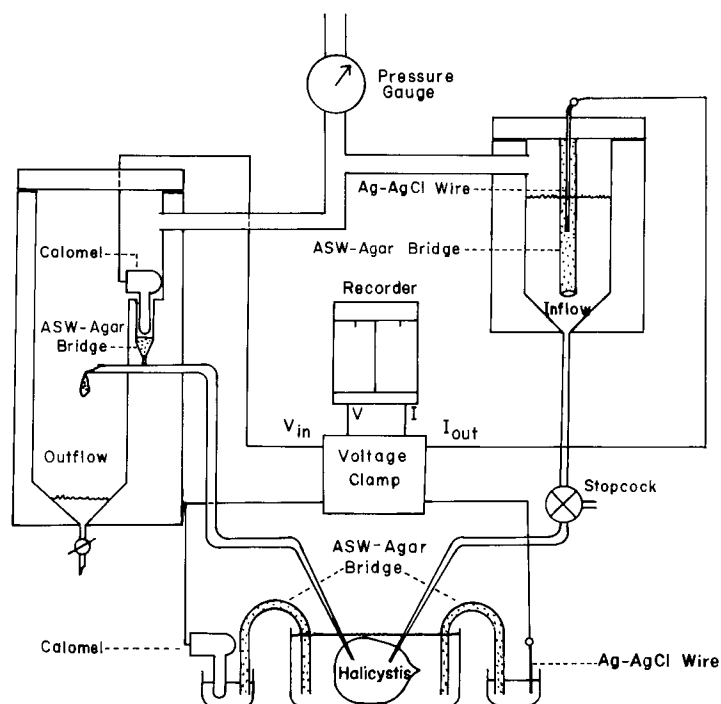


FIGURE 4. Diagram of system used for voltage clamping, vacuolar perfusion, and internal application of hydrostatic pressure.

protocol was generally applicable to influx experiments. After the short-circuit current (SCC) was reasonably steady, the external bath was exchanged for 4.0 ml of tracer-labeled ASW. The cell was then carefully raised off the chamber floor with the micromanipulators, thus exposing the total surface area to the solution. The bath was stirred periodically by repeatedly withdrawing and expelling a small portion. Each hour about 75 μl of H_2O were added to the bath to compensate for the known rate of evaporation. At 15-min intervals the perfusate was collected in a scintillation vial, weighed (to monitor perfusion rate), and counted in a scintillation counter. After allowing for an appropriate time to wash out the vacuole and dead volume (i.e., 15–30 min, depending upon the perfusion rate), three to five samples were taken, and at some point during the experiment three 10- μl samples of bath were counted to determine the specific activity (X^* in counts per minute per mole). The influx (J^{in}) was computed by:

$$J^{\text{in}} = P_i / (X^* \cdot A \cdot t), \quad (1)$$

where P_i is the mean count rate (cpm) in the perfusate samples for the sampling time interval t , and A is the surface area.

Chloride influx was measured with $^{36}\text{Cl}^-$ at an external concentration of 0.5–0.7 $\mu\text{Ci/ml}$. Sodium influx was measured with $^{22}\text{Na}^+$ at 3–5 $\mu\text{Ci/ml}$ in the bath. Potassium influx was measured with $^{42}\text{K}^+$ purchased as KOH from Nuclear Energy Services (NES), North Carolina State University, Raleigh, N.C. After neutralizing with HCl, an appropriate aliquot of the ^{42}KCl was added to K-free ASW to give 10 mM K^+ with 1.0–2.5 $\mu\text{Ci/ml}$.

The effluxes of Na^+ , K^+ , and Cl^- were measured in the following manner. After the tracer-labeled ASW was perfusing the vacuole, the external bath was replaced with 3.0 ml of fresh ASW, and two 0.6-ml aliquots of bath were taken as zero-time samples. The

sample volumes were replaced with fresh ASW. Three to four bath samples were taken at 30-min intervals, three 10- μ l aliquots of perfusate were counted to determine the vacuolar specific activity (X^*). The efflux (J^{out}) was calculated by:

$$J^{\text{out}} = P_o / (X^* \cdot A \cdot t), \quad (2)$$

where P_o is the mean change in total external radioactivity for sampling interval t .

Chloride efflux was measured with $^{36}\text{Cl}^-$ at 1.5–2.0 $\mu\text{Ci/ml}$. Sodium efflux was measured with $^{24}\text{Na}^+$ purchased from NES as NaOH. After neutralization with HCl, aliquots were added to ASW to give 2–8 $\mu\text{Ci/ml}$ without appreciably altering the Na^+ concentration. Potassium efflux was measured with $^{42}\text{K}^+$ as used in influx experiments.

Cell Wall Elastic Modulus

The elastic modulus for the cell wall was determined by measuring changes in cell volume at various internal hydrostatic pressures. The system shown in Fig. 4 was used to control the hydrostatic pressure difference between the vacuole and the bath. The thick-walled Lucite reservoir formed a gas-tight system in which the pressure generated by compressed N_2 was controlled with a needle valve attached to the tank regulator. In each experiment the diameter of a nearly spherical cell was measured with a calibrated micrometer eyepiece first at zero pressure and again 1–3 min after each test pressure was reached. The volumetric elastic modulus (ϵ in atm) was computed from the pressure-volume change relationship (32, 49):

$$P_f - P_i = \epsilon[(V_f/V_i) - 1], \quad (3)$$

where P_i and P_f are initial and final pressure, respectively, and V_i and V_f are the volumes at those pressures.

RESULTS

Electrical Properties and Ion Concentrations

In order to determine whether an ion is actively transported (pumped) or passively distributed across a membrane system, the electrical potential difference (PD) as well as the ion concentrations and fluxes must be known. The measured PD in *H. parvula* had two distinct phases. Upon penetration of the cell with the first microelectrode a PD between 0 and -90 mV (sign refers to vacuole with respect to bath) was recorded. For the next several minutes a steady hyperpolarization usually occurred. A final, steady value was usually reached within 15 min, although occasionally up to 90 min was required. The final PD's were consistently between -70 and -95 mV. Therefore, these values were used in the following analysis. This PD was -82.5 ± 1.3 (73). The surface resistance (R_s), which was measured at steady state values of PD, was $1,205 \pm 82$ (55) $\Omega \text{ cm}^2$.

We also desired to know the electrical properties of each membrane but found no satisfactory technique for knowingly placing the microelectrode tip in the thin cytoplasmic layer. Attempts at very careful impalement of the plasmalemma were thwarted by the high degree of elastic deformation of the cell wall as the electrode impinged upon it.

Table I shows the concentrations of the major cations present in vacuolar sap and in ASW. It is apparent that, except for pH, the sap cation composition is similar to that of the ASW, as was determined previously for *H. osterhoutii* (2). To ascertain whether these ions are actively or passively transported, we conducted

TABLE I
CONCENTRATIONS AND EQUILIBRIUM POTENTIALS FOR INORGANIC IONS IN THE VACUOLAR SAP OF *H. parvula*

Ion	Concentration in sap*	Concentration in ASW	Equilibrium potential‡	Electrochemical equilibrium potential ($\Delta\bar{\mu}_j$)
	mM	mM	mV	$10^3 J \cdot mol^{-1}$
K ⁺	9.2 ± 1.0 (30)	10.0	+2	-8.11
Na ⁺	415 ± 5 (22)	453	+2	-8.11
H ⁺	0.053 ± 0.005 (5)§	10 ⁻⁵	-220	+13.32
Ca ⁺⁺	42.1 ± 2.6 (12)	10.0	-18	-12.35
Mg ⁺⁺	65.3 ± 3.1 (12)	51.5	-3	-15.25
Cl ⁻	579 ± 8 (19)	530	+2	+8.15
Br ⁻	0.43 ± 0.002 (4)	1.0	-21	+5.88
NO ₃ ⁻	8.6 ± 0.7 (13)	0.1	+114	+18.91
H ₂ PO ₄ ⁻	0.323 ± 0.084 (10)	0.004	+112	+18.72
HPO ₄ ⁼	0.0011 ± 0.0003 (10)	0.046	-48	+6.56
SO ₄ ⁼	0.65 ± 0.10 (15)	26.5	-47	+6.75

* Data expressed as mean ± SE (number of samples).

‡ This value may be compared with the measured PD of -82 mV.

§ Computed from a pH of 4.3.

an electrochemical test for the passive distribution of each ion. The Ussing-Teorell flux ratio equation (43, 44) predicts the flux-force relationship for ions moving by independent diffusion. However, when the flux ratio is unity, the electrochemical distribution of a passively transported ion is defined by the familiar Nernst equation:

$$PD = E_j = \frac{RT}{z_j F} \ln \frac{{}^oC_j}{{}^iC_j}, \quad (4)$$

in which R , T , z_j , and F have their usual meanings, and oC_j and iC_j represent the external and internal concentrations of j , respectively. E_j is defined as the equilibrium potential for ion j .

Fig. 5 shows that the vacuolar concentrations of Na⁺, K⁺, and Cl⁻ remained essentially constant over 3 days in ASW. Thus, these cells were in approximate steady state, and we have assumed that the flux ratio for these ions is near unity. This assumption is reasonable for these monovalent ions for which the passive permeabilities are probably sufficiently high to nullify the potential pitfall associated with an appreciable growth rate (see 41). Thus for the passively distributed ion, $PD = E_j$, and any large deviation from this equality indicates active transport.

The electrochemical potential difference for ion ($\Delta\bar{\mu}_j$, joule mole⁻¹) is given by (see 18):

$$\Delta\bar{\mu}_j = z_j F (PD - E_j). \quad (5)$$

This equation yields the magnitude of the work necessary to maintain the nonequilibrium condition and the direction, vacuole to bath of the electrochemical gradient. If $\Delta\bar{\mu}_j$ is positive, the electrochemical potential is higher inside than outside, and active inward transport is suggested. Conversely, if $\Delta\bar{\mu}_j$ is negative, the ion is probably pumped out of the cell.

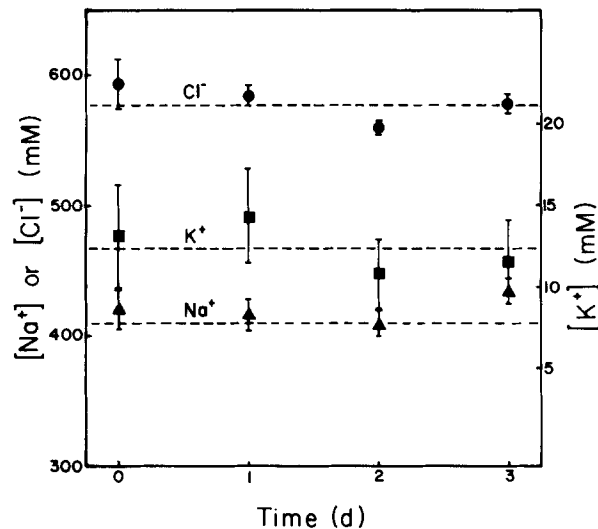


FIGURE 5. The vacuolar sap concentrations of Na^+ , K^+ , and Cl^- for 3 days after transfer from ESW to ASW. Points and bars are the mean \pm SE for five cells. Each dashed line represents the mean of all means for that ion.

Consideration of the $\Delta\bar{\mu}_j$ values for Na^+ and K^+ (Table I) indicates that both of these cations are pumped out of the vacuole. The same conclusion appears to be true for Ca^{++} and Mg^{++} , which show even greater values of $\Delta\bar{\mu}_j$. However, this interpretation for the divalent cations must be viewed with caution because a low passive permeability for Ca^{++} could account for the deviation from electrochemical equilibrium. For example, in growing cells of *Nitella translucens*, a freshwater alga, a low permeability to Ca^{++} combined with a large inward driving force resulted in a flux ratio much greater than one across the plasmalemma which probably accounted for the failure of the Nernst equation to predict the cytoplasmic $[\text{Ca}^{++}]$ (41). The sap H^+ also lies far out of equilibrium in the direction suggesting inward pumping, but there are other possible mechanisms, such as the secretion of organic acids, which could account for the low sap pH.

While an outwardly directed Na^+ pump is almost universal in plant and animal cells, an outwardly directed K^+ pump is unusual. The cytoplasmic $[\text{K}^+]$ in growing, reproductive cells is commonly much higher than that in the external medium. This led us to ask whether the cytoplasmic $[\text{K}^+]$ was much higher than the sap $[\text{K}^+]$, in which case the whole cell $[\text{K}^+]$ would be greater than that for isolated sap. Table II shows that there was, in fact, a significant difference of 8.9 mM between isolated sap and whole cells. With only 10 mM K^+ in the ASW, it is unlikely that the difference was due to external adsorption of K^+ by the cell wall. Since the cytoplasmic thickness varies from 5 to 15 μm (47), we used 10 μm to calculate a cytoplasmic $[\text{K}^+]$ of 424 mM for a cell with dimensions similar to those used in these experiments. This value is similar to that determined for the cytoplasm of *Valonia ventricosa* (16), and the red marine alga *Porphyra perforata* (7). All of these estimates are probably somewhat higher than the ground

TABLE II
ESTIMATION OF CYTOPLASMIC POTASSIUM CONCENTRATION IN *H. parvula*

Isolated sap [K ⁺]*	Whole cell [K ⁺]*	Significance (t test)	Cytoplasmic [K ⁺]‡
<i>mmol/liter sap</i>	<i>mmol/liter cell water</i>		<i>mmol/liter cytoplasm</i>
11.2 ± 1.4 (18)	20.1 ± 3.0 (16)	<i>P</i> < 0.005	424

* Data expressed as mean ± SE (number of cells).

‡ Calculated assuming a 10- μ m cytoplasmic thickness for a "typical" cell with dimensions of *a* = 4.0 mm, *b* = 2.5 mm (see Methods for details).

cytoplasm since they include the chloroplasts, and Larkum (28) showed that K⁺ is accumulated to high levels by chloroplasts.

Table I also shows the distribution of inorganic anions in the vacuolar sap of *H. parvula*. The principle anion in the sap is Cl⁻, and the large and positive $\Delta\bar{\mu}_j$ indicates an inward pump. Except for the few algal species with electropositive vacuoles (e.g., *Valonia*), all algae studied have inward Cl⁻ pumps (18, 30). As might be expected, the metabolized anions, NO₃⁻, SO₄⁻, and phosphate also appear to be actively transported into the cell. In a growing cell it is likely that the influx of a metabolized anion will be much greater than the efflux, which is the opposite to that predicted from electrochemical considerations. A flux ratio greater than one has been demonstrated for phosphate transport in *Nitella* (39) and *Hydrodictyon* (33), both freshwater algae. Thus, a positive $\Delta\bar{\mu}_j$ almost certainly indicates inward active transport, provided that the anion in the vacuolar sap remains inorganic. Comparison of the ³²P radiochromatogram for sap and H₂³²PO₄⁻ showed that 95–100% of the sap phosphate was inorganic, and no correction was made for the organic fraction. Phosphate was separated into the monovalent and divalent forms using the well-known Henderson-Hasselbalch equation with the known pH of the sap and ASW. Although both H₂PO₄⁻ and HPO₄⁻ have a positive $\Delta\bar{\mu}_j$, only one form needs to be actively transported to give this result. Comparison of ³⁵S radiochromatograms showed that about 20% of the sap ³⁵S was not ³⁵SO₄⁻, so this fraction was subtracted from the total to give the value shown in Table I.

The total equivalents of inorganic cations and anions computed from the data in Table I are 639.1 ± 4.1 and 589.1 ± 3.5 meq/liter, respectively. There is a significant excess of cations (*P* < 0.005) of about 50 meq/liter. Except for trace elements, all of the important inorganic ions are represented in Table I. At pH 4.3 the HCO₃⁻ concentration is negligible, so the discrepancy between cations and anions is probably due to the presence of organic anions. For example, Saddler (35) found 110 mM oxalate in the vacuolar sap of *Acetabularia*.

Short-Circuit Current Analysis

The large size of *Halicystis* cells allowed the vacuole to be perfused with solutions of any desired composition, and it was therefore possible to bathe both sides of the protoplast with the same ASW solution. The short-circuit current technique developed by Ussing and Zerahn (45) requires that all ionic gradients across the membrane system be abolished, and any remaining PD be nulled or short-

circuited to zero. Under these conditions Ginzburg and Hogg (13) theoretically demonstrated that a stable short-circuit current (SCC) developed as a consequence of abolishing the PD is a direct measure of the algebraic sum of the net active ion transports. Furthermore, under short-circuit conditions any net flux of an ion must be due to the active transport of that ion.

When the vacuole of *H. parvula* was perfused and bathed with ASW, a new, steady PD of -50 to -65 mV was usually reached within 20–60 min. After clamping the PD at zero the SCC normally became steady within 30–60 min. Table III shows the flux values for Na^+ , K^+ , and Cl^- , as well as the mean SCC for each set of experiments. The SCC for the 28 cells used in all flux experiments was 299 ± 24 $\text{peq} \cdot \text{cm}^{-2} \cdot \text{s}^{-1}$ or about $29 \mu\text{A} \cdot \text{cm}^{-2}$, which is not significantly different from the net Cl^- influx of about $290 \text{ pmol} \cdot \text{cm}^{-2} \cdot \text{s}^{-1}$. There was a significant net K^+ efflux of $0.65 \text{ pmol} \cdot \text{cm}^{-2} \cdot \text{s}^{-1}$, while the Na^+ fluxes were not significantly different. Fig. 6 shows that the unidirectional Cl^- influx is proportional to the SCC over the range of variation with a linear regression slope of

TABLE III
ION FLUXES AND SHORT-CIRCUIT CURRENT IN *H. parvula* CELLS
INTERNALLY PERFUSED WITH ASW

Ion	Influx*	Efflux*	Net Flux‡	Significance for net flux (<i>t</i> test)	SCC*§
	$\text{pmol} \cdot \text{cm}^{-2} \cdot \text{s}^{-1}$	$\text{pmol} \cdot \text{cm}^{-2} \cdot \text{s}^{-1}$	$\text{pmol} \cdot \text{cm}^{-2} \cdot \text{s}^{-1}$		$\text{peq} \cdot \text{cm}^{-2} \cdot \text{s}^{-1}$
Cl^-	354 ± 59 (9)	64.3 ± 14.6 (4)	-290 ± 49	$P \ll 0.005$	313 ± 42 (13)
Na^+	38.7 ± 9.0 (5)	46.1 ± 7.1 (4)	$+7.4 \pm 8.2$	$P > 0.10$	299 ± 41 (9)
K^+	0.82 ± 0.07 (3)	1.47 ± 0.30 (3)	$+0.65 \pm 0.22$	$P < 0.025$	268 ± 24 (6)

* Data expressed as mean \pm SE (number of cells).

‡ Direction indicated by sign; outward (+), inward (-).

§ The SCC measured during flux experiments for each ion.

|| Converted to these units by: $(\mu\text{A cm}^{-2})/(F \times 10^4)$.

1.12. From this analysis we conclude that Cl^- is actively transported into the vacuole and that the SCC is a good measure of the rate of active transport of Cl^- .

Turgor Pressure and Cell Wall Elastic Modulus

The osmolality of the vacuolar sap was measured in two experiments with a total of five sap samples. The osmolality difference between the sap and the ASW in which the cells were pretreated was 23 ± 6 mosmol/kg. The osmotic pressure difference ($\Delta\Pi$ in atm) was estimated by the van't Hoff equation (see 27):

$$\Delta\Pi = R \cdot T \cdot \Delta C, \quad (6)$$

where ΔC is the osmolal concentration difference. Thus, the mean osmotic pressure difference is 0.54 atm. Assuming that the net flow of water is essentially zero, this osmotic pressure difference is equal to the hydrostatic pressure difference or turgor pressure. Turgor pressures for most vacuolated marine algae range from 1.5 to 13 atm (see 24). The value for *H. parvula* is therefore unusually low but is, nevertheless, in agreement with the earlier values of 0.25–0.5 atm reported for *Halicystis* (1, 20).

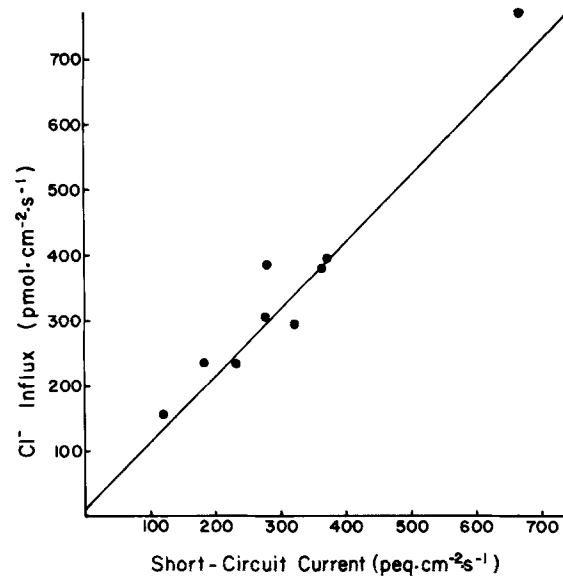


FIGURE 6. Relationship between unidirectional Cl^- influx and SCC in perfused cells. Each point corresponds to the mean value of Cl^- influx and SCC in a single cell under standard conditions. The line is a least squares regression with a slope of 1.12, $r = 0.98$ ($N = 9$).

When the turgor pressure of a cell was reduced (e.g., upon removing a microelectrode) we observed a conspicuous decrease in the cell volume, which suggested an unusually low degree of wall rigidity. Dainty et al. (6) demonstrated that the elastic modulus of a cell wall is an important parameter in the osmotic relations of plant cells. Therefore, in order to estimate the elastic modulus (ϵ in atm) for the cell wall we determined the change in cell volume as a function of internally applied pressure (Fig. 7). The slope of the nearly linear curve in Fig. 7 is about 1.7 atm^{-1} . From Eq. 4 (see Methods section), we found that the value of ϵ (the reciprocal of this slope) was 0.6 atm .

DISCUSSION

Steady-State Ionic Distribution

We have measured the concentrations of all inorganic ions in the vacuolar sap of *H. parvula*. Assuming that the cells were in a steady state, we calculated the equilibrium potential of each ion and compared it to the measured PD (-82 mV) to determine the existence and direction of active transport. This analysis indicates that Na^+ and K^+ and all anions are actively transported.

The electrochemical analysis for vacuolar K^+ (Table I) and the observed net efflux of K^+ under short-circuit conditions both indicate that this ion is pumped out of the vacuole. The concentration of K^+ in the cytoplasm is about 45 times that in the vacuolar sap (Table II). Without knowing the potential difference across each membrane, the location of the outward K^+ pump cannot be assigned

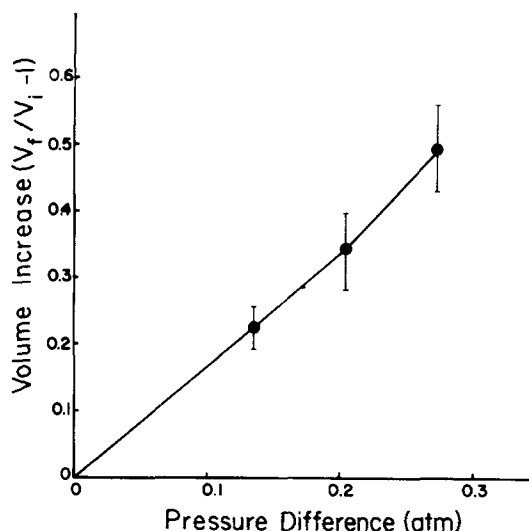


FIGURE 7. Increase in cell volume as a function of internally applied hydrostatic pressure; V_i is the volume at zero pressure. V_f is the final volume. Points and bars represent the mean \pm SE for four to five cells.

with certainty. However, a passive distribution of K^+ across the tonoplast would require an unusual combination of membrane potentials (e.g., -170 mV at the plasmalemma and $+90$ mV at the tonoplast). Thus, it seems more likely that the outward K^+ pump is located at the tonoplast. The most common mechanism for maintaining a high $[K^+]$ in the cytoplasm in both plant and animal cells is an inward pump at the plasmalemma, which is often associated with outward Na^+ transport. Such an inward K^+ pump at the plasmalemma of *H. parvula* is not ruled out by the evidence presented.

Electrochemical evidence indicates that Na^+ is also pumped out of the vacuole (Table I). Since the $[K^+]$ in the cytoplasm is probably more than 300 mM, for osmotic stability the $[Na^+]$ in the cytoplasm must be no greater than about one-half the $[Na^+]$ in the vacuolar sap. Without knowing the electrical potential across the tonoplast an inward Na^+ pump cannot be assigned to that membrane with certainty. Nevertheless, an inward Na^+ pump at the tonoplast in addition to an outward Na^+ pump at the plasmalemma with a similar pumping rate could explain the lack of a net Na^+ efflux under short-circuit conditions. In such a system the passive Na^+ fluxes could be much smaller than the active Na^+ fluxes and would not then contribute significantly to the flux ratio under any experimental conditions. There is good evidence for an inward Na^+ pump at the tonoplast in *Nitella* (40) and in *Valonia* (16). It therefore is possible that Na^+ and K^+ are transported in opposite directions at each membrane of *H. parvula*.

We have presented evidence that all inorganic anions are actively transported into the cell (Table I). In addition, the large net influx of Cl^- under short-circuit conditions (Table III) unequivocally indicates active Cl^- transport. Only those algae with electropositive vacuoles, namely *Valonia* (16) and *Chaetomorpha* (8),

appear to lack Cl^- pumps. With regard to the metabolized anions, NO_3^- , $\text{SO}_4^{=}$, and phosphate, there are only a few studies in vacuolated algae which deal with the transport of these ions. Jacques and Osterhout (21) found that NO_3^- was concentrated in the sap of *Valonia macryophysa* by 2,000-fold and in the sap of *H. osterhoutii* by 500-fold over the concentration in natural seawater, which is less than $10 \mu\text{M}$. The accumulation of phosphate and $\text{SO}_4^{=}$ has been shown in several species of marine algae (23, 24, 35). Likewise, the active inward transport of phosphate (33, 39) and of $\text{SO}_4^{=}$ (34) has been demonstrated in freshwater algae.

With no estimation of the cytoplasmic concentrations of these anions, it is impossible to assign the locations of their pumps. However, in the freshwater algae (30) and in *Acetabularia* (36) the Cl^- pump is located at the plasmalemma. It also is likely that the pumps for the metabolized anions reside at the plasmalemma because a high concentration in the cytoplasm would be metabolically advantageous. Good electrochemical data for the freshwater alga, *Hydrodictyon*, indicate that the phosphate pump is indeed at the plasmalemma in this cell (33).

The Short-Circuit Current

In cells of *H. parvula* perfused with ASW the mean SCC is $299 \text{ peq} \cdot \text{cm}^{-2} \cdot \text{s}^{-1}$ (ca. $29 \mu\text{A} \cdot \text{cm}^{-2}$). The net Cl^- influx of $290 \text{ peq} \cdot \text{cm}^{-2} \cdot \text{s}^{-1}$ is not statistically different from the mean SCC, and the unidirectional Cl^- influx is proportional to the SCC over the range of variability (Fig. 6). There is no statistically significant net Na^+ flux, and the net K^+ efflux is trivial compared to the net Cl^- flux (Table III). Therefore, virtually all of the SCC is generated by the active transport of Cl^- into the cell.

In *H. ovalis* the mean SCC computed from the data of Blount and Levedahl (3) is identical to the value determined for *H. parvula*. However, in *H. ovalis* about 39% of the SCC is due to a net Na^+ efflux, and the remainder is due to net Cl^- influx. Thus, the fact that the SCC for both species is identical is probably fortuitous.

The SCC has been measured in only two other plant cells. In *Valonia ventricosa* Gutknecht (17) found an SCC of about $100 \text{ peq} \cdot \text{cm}^{-2} \cdot \text{s}^{-1}$. This SCC is nearly accounted for by the large net influx of K^+ and a smaller net influx of Na^+ . In *Nitella clavata* the SCC is only about $18 \text{ peq} \cdot \text{cm}^{-2} \cdot \text{s}^{-1}$, and the ionic origin is unknown (42). Thus, in *Halicystis* the SCC is appreciably greater than the values reported for other plant cells and is more like the SCC's generated by some animal epithelia (see 25).

H. parvula (and *H. osterhoutii*) may be uniquely suited to a short-circuit current analysis of ion transport. In other plant and animal preparations used for this purpose the solutions bathing the two sides of the "membrane" are normally quite different in ionic composition, and at least one of the solutions must be substantially altered in order to attain symmetrical or short-circuit conditions. However, except for pH, the vacuolar sap of *H. parvula* is similar in ionic composition to the external seawater. Thus, with *H. parvula* the short-circuit current analysis of ion transport may be more relevant to the intact cell than with any system previously used.

Osmotic Relations and Elastic Properties of the Cell Wall

The existence of a turgor pressure in walled plant cells appears to be universal. Unlike animal cells, most plant cells have an external cell wall capable of withstanding appreciable hydrostatic pressure. Turgor pressure appears to play a critical role in maintaining normal cell growth and must therefore be regarded as a physiologically important parameter (15). The turgor pressure of *H. parvula* is about 0.5 atm, which is in agreement with previous determinations for *Halicystis* (1, 20). This pressure is lower than those in most other walled algae, which usually range from 1.5 to 13 atm.

The cell wall of *H. parvula* has an unusually low elastic modulus (i.e., low degree of rigidity). Table IV shows the volumetric elastic moduli (ϵ) for the cell walls of *H. parvula* and three other algae which were determined at similar pressures. It is apparent that the ϵ for *H. parvula* is at least two orders of magnitude lower than that of any other alga. This low elastic modulus is consistent with the observation by Jacques (20) that the cell volume of *H. osterhoutii* decreased by an appreciable amount when it was impaled with a glass pipet.

TABLE IV
VOLUMETRIC ELASTIC MODULI OF THE CELL WALLS OF SEVERAL ALGAE
DETERMINED AT LOW PRESSURES

Alga	Habitat	Elastic modulus	Pressure range	Reference
			of measurement	
		atm	atm	
<i>Nitella flexilis</i>	Freshwater	67	0-1.0	(22)
<i>Valonia ventricosa</i>	Marine	182	0-1.0	(46)
<i>Valonia utricularis</i>	Marine	90	0-0.5	(49)
<i>Halicystis parvula</i>	Marine	0.6	0-0.4	Present study

Zimmermann and Steudle (49, 50) recently demonstrated that the elastic moduli of *V. utricularis* and *N. flexilis* are dependent on the turgor pressure when the determination is made at pressures below 2 atm. Furthermore, these investigators found ϵ was also proportional to the total cell volume (50). For *V. utricularis* ϵ ranged from 125 to 300 atm at pressures (i.e., 3-6 atm) at which the value of ϵ is independent of pressure. The analogous range of ϵ for *N. flexilis* was 100-200 atm. Also, Dainty et al. (6) have estimated the pressure-independent ϵ for one size range of *Chara corallina* to be around 700 atm. Because the applied pressures used in this study were quite small, it is likely that the ϵ determined for *H. parvula* falls within the pressure-dependent region. The highly extensible wall of *H. parvula* often leads to breakage of the seals around the pipets at pressures greater than 0.5 atm, and therefore it may be difficult or impossible to accurately measure the pressure-independent ϵ by this technique. However, the value of ϵ which exists at pressures near the normal turgor pressure (i.e., 0.5 atm for *H. parvula*) has the greatest physiological significance, and the ϵ of 0.6 atm determined at pressures up to 0.4 atm is relevant in this regard. Also, we did not attempt to determine the cell volume to ϵ relationship for *H. parvula*. All of the determinations in this work were made on cells between 35 and 60 mm^3 in

volume, so the value of 0.6 atm is relevant only to cells in this size range.

The molecular interactions involved in determining the elastic properties of cell walls are not well understood. However, it is noteworthy that the chemical composition of the walls of *Halicystis* and a few close relatives is also unusual. In addition to the common structural component, cellulose, *Halicystis* walls contain polyxylan as the major structural polysaccharide (10). Unlike cellulose, the xylan chains are helically coiled (11). There is undoubtedly a relation between molecular structure and extensibility, but that relationship remains to be determined.

Send reprint requests to Dr. Gutknecht, Duke Marine Laboratory, Beaufort, N. C. 28516.

We thank Mr. M. Bradley for providing technical assistance and Ms. M. Bisson for critically reading the manuscript.

Dr. D. Hastings designed and assembled the apparatus used for vacuolar perfusion experiments.

The first author (J. S. G.) was supported by a predoctoral traineeship from N. I. H.

This work was supported by U.S.P.H.S. Grant HL12157.

Received for publication 31 July 1975.

REFERENCES

1. BLINKS, L. R. 1951. Physiology and Biochemistry of the Algae. In *Manual of Phycology*. G. M. Smith, editor. Cronica Botanica Co., Waltham, Mass. 263-290.
2. BLINKS, L. R., and A. G. JACQUES. 1930. The cell sap of *Halicystis*. *J. Gen. Physiol.* **13**:733-737.
3. BLOUNT, R. W., and B. H. LEVEDAHL. 1960. Active sodium and chloride transport in the single celled marine alga, *Halicystis ovalis*. *Acta Physiol. Scand.* **49**:1-9.
4. BROOKS, S. C. 1930. Composition of the cell sap of *Halicystis ovalis*. (Lyng.) Areschoug. *Proc. Soc. Exp. Biol. Med.* **27**:409-412.
5. CHAPMAN, V. J. 1962. *The Algae*. MacMillan and Co. Ltd., London.
6. DAINTY, J., H. VINTERS, and M. T. TYREE. 1974. A study of transcellular osmosis and the kinetics of swelling and shrinking in cells of *Chara corallina*. In *Membrane Transport in Plants*. U. Zimmermann and J. Dainty, editors. Springer-Verlag, New York. 59-63.
7. EPPLEY, R. W., and L. R. BLINKS. 1957. Cell space and apparent free space in the red alga, *Porphyra perforata*. *Plant Physiol.* **32**:63-64.
8. FINDLAY, G. P., A. B. HOPE, M. G. PITMAN, E. A. SMITH, and N. A. WALKER. 1971. Ionic relations of marine algae. III. Chaetomorpha: Membrane electrical properties and chloride fluxes. *Aust. J. Biol. Sci.* **24**:731-745.
9. FISKE, C. H., and Y. SUBBAROW. 1925. The colorimetric determination of phosphorus. *J. Biol. Chem.* **66**:375-400.
10. FREI, E., and R. D. PRESTON. 1961. Variants in the structural polysaccharides of algal cell walls. *Nature (Lond.)* **192**:939-943.
11. FREI, E., and R. D. PRESTON. 1964. Non-cellulosic structural polysaccharides in algal cell walls. I. Xylan in siphonous green algae. *Proc. R. Soc. Lond. B Biol. Sci.* **160**:293-313.
12. GAGE, P. W., and R. S. EISENBERG. 1969. Capacitance of the surface and transverse tubular membrane of frog sartorius muscle fibers. *J. Gen. Physiol.* **53**:265-278.
13. GINZBURG, B. Z., and J. HOGG. 1967. What does a short-circuit current measure in biological systems? *J. Theor. Biol.* **14**:316-322.

14. GRAVES, J. S. 1974. Ion transport and electrical properties of the marine alga, *Halicystis parvula*. Ph.D. Dissertation. Duke University, Durham, N. C.
15. GREEN, P. B., R. O. ERICKSON, and J. BUGGY. 1971. Metabolic and physical control of cell elongation rate. *Plant Physiol.* **47**:423-430.
16. GUTKNECHT, J. 1966. Sodium, potassium and chloride transport and membrane potentials in *Valonia ventricosa*. *Biol. Bull. (Woods Hole)*. **130**:331-344.
17. GUTKNECHT, J. 1967. Ion fluxes and short-circuit current in internally perfused cells of *Valonia ventricosa*. *J. Gen. Physiol.* **50**:1821-1834.
18. GUTKNECHT, J. and J. DAINTY. 1968. Ionic relations of marine algae. *Oceanogr. Mar. Biol. Annu. Rev.* **6**:163-200.
19. HANES, C. S., and F. A. ISCHERWOOD. 1949. Separation of the phosphoric esters on the filter paper chromatogram. *Nature (Lond.)*. **164**:1107-1112.
20. JACQUES, A. G. 1939. The kinetics of penetration. XIX. Entrance of electrolytes and of water into impaled *Halicystis*. *J. Gen. Physiol.* **22**:757-773.
21. JACQUES, A. G., and W. J. V. OSTERHOUT. 1938. The accumulation of electrolytes. XI. Accumulation of nitrate by *Valonia* and *Halicystis*. *J. Gen. Physiol.* **21**:767-773.
22. KAMIYA, N., M. TAWAWA, and T. TAKATA. 1963. The relation of turgor pressure to cell volume in *Nitella* with special reference to mechanical properties of the cell wall. *Protoplasma*. **57**:501-521.
23. KESSELER, H. 1964. Zellsaftgewinnung, AFS and Vakuolenkonzentration der osmotisch wichtigsten mineralischen Bestandteile einiger Helgölander Meeresalgen. *Helgol. Wiss. Meeresunters.* **11**:258-269.
24. KESSELER, H. 1965. Turgor, osmotisches potential und ionale zusammensetzung des Zellsaftes einiger Meeresalgen verschiedener verbreitungsgebiete. In *Proceedings of the Fifth Marine Biological Symposium, Botanica Gothoburgensia*. **3**:103-111.
25. KEYNES, R. D. 1969. From frog skin to sheep rumen: A survey of transport of salts and water across multicellular structures. *Q. Rev. Biophys.* **2**:177-281.
26. KORNMANN, P. 1938. Zur entwicklungsgeschichte von *Derbesia* und *Halicystis*. *Planta (Berl.)*. **28**:464-470.
27. KOTYK, A., and K. JANACEK. 1970. Cell Membrane Transport. Plenum Press, New York.
28. LARKUM, A. W. D. 1968. Ionic relations of chloroplasts in vivo. *Nature (Lond.)*. **218**:447-449.
29. LOWE, R. H., and H. J. EVANS. 1964. Preparation and some properties of a soluble nitrate reductase from *Rhizobium japonicum*. *Biochim. Biophys. Acta.* **85**:377-389.
30. MACROBBIE, E. A. C. 1970. The active transport of ions in plant cells. *Q. Rev. Biophys.* **3**:251-294.
31. PAGE, J. Z. 1970. Existence of a *Derbesia* phase in the life history of *Halicystis osterhoutii* Blinks and Blinks. *J. Phycol.* **6**:375-380.
32. PHILIP, J. R. 1958. The osmotic cell, solute diffusibility and the plant water economy. *Plant Physiol.* **33**:264-275.
33. RAVEN, J. A. 1974. Phosphate transport in *Hydrodictyon africanum*. *New Phytol.* **73**:421-432.
34. ROBINSON, J. B. 1969. Sulfate influx in characean cells. I. General characteristics. *J. Exp. Bot.* **20**:201-211.
35. SADDLER, H. D. W. 1970. The ionic relations of *Acetabularia mediterranea*. *J. Exp. Bot.* **21**:345-359.

36. SADDLER, H. D. W. 1970. The membrane potential of *Acetabularia mediterranea*. *J. Gen. Physiol.* **55**:802-821.
37. SANUI, S., and N. PACE. 1966. Application of atomic absorption in the study of Na, K, Mg and Ca binding by cellular membranes. *Appl. Spectrosc.* **20**:135-141.
38. SEARS, J. R., and R. T. WILCE. 1970. Reproduction and systematics of the marine alga *Derbesia* (Chlorophyceae) in New England. *J. Phycol.* **6**:381-392.
39. SMITH, F. A. 1966. Active phosphate uptake by *Nitella translucens*. *Biochim. Biophys. Acta.* **126**:94-99.
40. SPANSWICK, R. M., and E. J. WILLIAMS. 1964. Electrical potentials and Na, K, and Cl concentrations in the vacuole and cytoplasm of *Nitella translucens*. *J. Exp. Bot.* **15**:193-200.
41. SPANSWICK, R. M., and E. J. WILLIAMS. 1965. Ca fluxes and membrane potentials in *Nitella translucens*. *J. Exp. Bot.* **16**:463-473.
42. STRUNK, T. H. 1971. Correlation between metabolic parameters of transport and vacuolar perfusion results in *Nitella clavata*. *J. Exp. Bot.* **22**:863-874.
43. TEORELL, T. 1949. Membrane electrophoresis in relation to bioelectric polarization effects. *Arch. Sci. Physiol.* **3**:205-219.
44. USSING, H. H. 1949. The distinction by means of tracers between active transport and diffusion. *Acta Physiol. Scand.* **19**:43-56.
45. USSING, H. H., and K. ZERAHN. 1950. Active transport of sodium as the source of electric current in the short-circuited isolated frog skin. *Acta Physiol. Scand.* **23**:110-127.
46. VILLEGAS, L. 1967. Changes in volume and turgor pressure in *Valonia* cells. *Biochim. Biophys. Acta.* **136**:590-593.
47. WHEELER, A. E. and J. Z. PAGE. 1974. The ultrastructure of *Derbesia tenuissima*. I. Organization of the gametophyte protoplast, gametangium, and gametangial pore. *J. Phycol.* **10**:336-352.
48. ZIEGLER, J. R. and J. M. KINGSBURY. 1964. Cultural studies on the marine green alga *Halicystis parvula-Derbesia tenuissima*. I. Normal and abnormal sexual and asexual reproduction. *Phycologia.* **4**:105-116.
49. ZIMMERMANN, U., and E. STEUDLE. 1974. The pressure-dependence of the hydraulic conductivity, the membrane resistance and the membrane potential during turgor pressure regulation in *Valonia utricularis*. *J. Membr. Biol.* **16**:331-352.
50. ZIMMERMANN, U., and E. STEUDLE. 1974. Hydraulic conductivity and volumetric elastic modulus in giant algal cells: pressure and volume dependence. In *Membrane Transport in Plants*. U. Zimmermann and J. Dainty, editors. Springer-Verlag, New York. 64-71.